HHS Public Access

Author manuscript

Gastroenterology. Author manuscript; available in PMC 2015 November 03.

Published in final edited form as:

Gastroenterology. 2010 July ; 139(1): 323–34.e7. doi:10.1053/j.gastro.2010.03.052.

Toll-Like Receptor 9 Promotes Steatohepatitis by Induction of Interleukin-1β in Mice

KOUICHI MIURA[*,‡], **YUZO KODAMA**[*], **SAYAKA INOKUCHI**[*], **BERND SCHNABL**[*], **TOMONORI AOYAMA**[*], **HIROHIDE OHNISHI**[‡], **JERROLD M. OLEFSKY**[*], **DAVID A. BRENNER**[*], and **EKIHIRO SEKI**[*]

[*]Department of Medicine, University of California, San Diego, School of Medicine, La Jolla, California

[‡]Department of Gastroenterology, Akita University Graduate School of Medicine, Akita, Japan

Abstract

BACKGROUND & AIMS—Development of nonalcoholic steatohepatitis (NASH) involves the innate immune system and is mediated by Kupffer cells and hepatic stellate cells (HSCs). Toll-like receptor 9 (TLR9) is a pattern recognition receptor that recognizes bacteria-derived cytosine phosphate guanine (CpG)–containing DNA and activates innate immunity. We investigated the role of TLR9 signaling and the inflammatory cytokine interleukin-1β (IL-1β) in steatohepatitis, fibrosis, and insulin resistance.

METHODS—Wild-type (WT), TLR9$^{-/-}$, IL-1 receptor (IL-1R)$^{-/-}$, and MyD88$^{-/-}$ mice were fed a choline-deficient amino acid-defined (CDAA) diet for 22 weeks and then assessed for steatohepatitis, fibrosis, and insulin resistance. Lipid accumulation and cell death were assessed in isolated hepatocytes. Kupffer cells and HSCs were isolated to assess inflammatory and fibrogenic responses, respectively.

RESULTS—The CDAA diet induced NASH in WT mice, characterized by steatosis, inflammation, fibrosis, and insulin resistance. TLR9$^{-/-}$ mice showed less steatohepatitis and liver fibrosis than WT mice. Among inflammatory cytokines, IL-1β production was suppressed in TLR9$^{-/-}$ mice. Kupffer cells produced IL-1β in response to CpG oligodeoxynucleotide. IL-1β but not CpG-oligodeoxynucleotides, increased lipid accumulation in hepatocytes. Lipid accumulation in hepatocytes led to nuclear factor-κB inactivation, resulting in cell death in response to IL-1β. IL-1β induced fibrogenic responses in HSCs, including secretion of tissue inhibitor of metalloproteinase-1. IL-1R$^{-/-}$ mice had reduced steatohepatitis and fibrosis, compared with WT mice. Mice deficient in MyD88, an adaptor molecule for TLR9 and IL-1R signaling, also had

Address requests for reprints to: Ekihiro Seki, MD, PhD, Division of Gastroenterology, Department of Medicine, University of California San Diego, School of Medicine, Leichtag Biomedical Science Building Room #349I, 9500 Gilman Drive, La Jolla, CA 92093. ekseki@ucsd.edu; fax: (858) 822-5370. Or to Kouichi Miura, MD, PhD, Department of Gastroenterology, Akita University Graduate School of Medicine, 1-1-1 Hondo Akita-shi, Akita, Japan 010-8543. miura116@doc.med.akita-u.ac.jp; fax; (81) 18-836-2611.

Conflicts of interest

The authors disclose no conflicts.

Supplementary Material

Note: To access the supplementary material accompanying this article, visit the online version of *Gastroenterology* at www.gastrojournal.org, and at doi: 10.1053/j.gastro.2010.03.052.

reduced steatohepatitis and fibrosis. TLR9$^{-/-}$, IL-1R$^{-/-}$, and MyD88$^{-/-}$ mice had less insulin resistance than WT mice on the CDAA diet.

CONCLUSIONS—In a mouse model of NASH, TLR9 signaling induces production of IL-1β by Kupffer cells, leading to steatosis, inflammation, and fibrosis.

Keywords

Nonalcoholic Fatty Liver Diseases; Toll-Like Receptors; Bacterial DNA; Bambi

Nonalcoholic fatty liver disease (NAFLD) is one of the most common liver diseases in the United States and is becoming a significant public health concern worldwide. NAFLD is a hepatic component of the metabolic syndrome, which is characterized by visceral fat accumulation, insulin resistance, dyslipidemia, and hypertension.[1,2] Although NAFLD is generally a benign liver disease, a subset of NAFLD includes progressive liver disease designated nonalcoholic steatohepatitis (NASH). An emerging concept is that the innate immune system mediates the development of NASH.[3] In NASH, Kupffer cells, hepatic resident macrophages, are the primary cells that produce various inflammatory and fibrogenic mediators, which involve the activation of hepatic stellate cells (HSCs).[4] Activated HSCs produce chemokines, cytokines, and excessive extracellular matrix, resulting in fibrosis.[5,6]

As a component of the innate immune system, Toll-like receptors (TLRs) recognize highly conserved microbial structures as pathogen-associated molecular patterns such as lipopolysaccharide (LPS).[7] Thirteen TLRs have been identified in mammals for host defense against microorganisms. TLRs, except for TLR3, use MyD88, an essential adaptor molecule, to activate transcription factors, such as nuclear factor-κB (NF-κB), activator protein 1 (AP-1), and interferon regulatory factors that induce inflammatory cytokines and interferon-inducible genes.[7] TLRs are associated with liver diseases, including alcoholic liver injury, ischemic-reperfusion injury, liver fibrosis, and liver cancer.[8–10] Indeed, mice mutated in TLR4 and MyD88 are resistant to liver damage and fibrosis both in toxin-induced and cholestasis-induced liver injury.[10,11] Thus, the TLR-MyD88 pathway plays an important role in liver injury and fibrosis as well as host defense.

TLR9 is a receptor for unmethylated cytosine phosphate guanine (CpG)–containing DNA, a major component of bacterial DNA.[7,12] In chronic liver disease, bacterial DNA is often detected in blood and ascites in both rodents and human beings.[13,14] Host-derived denatured DNA from apoptotic cells is also recognized by TLR9 as an endogenous ligand.[15,16] Thus, liver cells might be exposed to high levels of TLR9 ligands after liver injury. Indeed, TLR9$^{-/-}$ mice exhibit reduced liver injury and fibrosis induced by carbon tetrachloride, acetaminophen, and bile duct ligation, indicating that TLR9 plays a crucial role in liver diseases.[15–17] However, the role of TLR9 in the development of NASH is unknown.

The present study investigated the role of TLR9 and downstream signaling in the setting of steatohepatitis induced by a choline-deficient amino-acid defined (CDAA) diet. We show that TLR9 expression in Kupffer cells and subsequent interleukin-1β (IL-1β) production are important for the development of NASH.

Materials and Methods

Animals

Wild-type (WT) C57BL/6 mice and IL-1 receptor (IL-1R) $^{-/-}$ mice were purchased from Jackson Laboratories (Bar Harbor, ME). TLR9$^{-/-}$ and MyD88$^{-/-}$ mice backcrossed at least 10 generations onto the C57BL/6 background were a gift from Dr Akira (Osaka University, Japan).[12,18] These null mice exhibited similar hepatobiliary phenotypes and hepatic lipid contents when fed standard laboratory chow (Supplementary Table 1). Male mice were divided into 3 groups at 8 weeks old; standard chow group (PicoLab Rodent Diet 20 series, Catalog no. 5053; LabDiet, Framingham, MA); choline-supplemented L-amino acid defined diet (CSAA; catalog no. 518754; Dyets Inc, Bethlehem, PA); and choline-deficient L-amino acid defined diet (catalog no. 518753; Dyets Inc).[19] Both CSAA and CDAA diets contain higher calories than standard chow (Supplementary Table 2). These diets were continued for 22 weeks. In some experiments, Kupffer cells were depleted by liposomal clodronate.[11,20] Briefly, 200 μL of liposomal clodronate was injected into the mice intravenously after 21 weeks of CDAA diet feeding, and then mice were killed 1 week later. The food intake on the CDAA diet was monitored for 1 month. The mice received humane care according to US National Institutes of Health (NIH) recommendations outlined in the “Guide for the Care and Use of Laboratory Animals.” All animal experiments were approved by the University of California San Diego Institutional Animal Care and Use Committee.

Histologic Examination

H&E, Oil-Red O, TdT (terminal deoxynucleotidyl-transferase)–mediated dUTP (2′-deoxyuridine 5′-triphosphate)–biotin neck end labeling (TUNEL), and Sirius red staining were performed.[11,21] TUNEL-positive cells were counted on 10 high power (400×) fields/slide. The Sirius red–positive area was measured on 10 low power (40×) fields/slide and quantified with the use of NIH imaging software. NAFLD activity score was determined as described.[22] Immunohistochemistry for F4/80, desmin, and CD31 was performed.[11]

Quantitative Real-Time Polymerase Chain Reaction Analysis

Extracted RNA from livers and cells was subjected to reverse transcription and subsequent quantitative real-time polymerase chain reaction (PCR) with the use of ABI PRISM 7000 Sequence Detector (Applied Biosystems).[11] PCR primer sequences are listed in Supplementary Table 3. Genes were normalized to 18S RNA as an internal control.

Lipid Isolation and Measurement

Triglyceride, total cholesterol, and free fatty acid contents were measured with the use of Triglyceride Reagent Set (Pointe Scientific, Canton, MI), Cholesterol E (Wako, Richmond, VA), free fatty acid, and half micro test (Roche, Mannheim, Germany).

Assessment of Insulin Resistance

Homeostasis model assessment of insulin resistance (HOMA-IR) was calculated as [immunoreactive insulin (μU/mL) × fasting blood sugar (mg/dL) ÷ 405].[23]

Cell Isolation and Treatment

Hepatocytes, HSCs, and Kupffer cells were isolated from mice as previously described.[11,21] After cell attachment, hepatocytes were serum starved for 16 hours. The culture media for Kupffer cells and HSCs were changed to 1% serum for 16 hours followed by treatment with 10 ng/mL IL-1*β*, 5 *μ*g/mL CpG-oligodeoxynucleotide (ODN; ODN1826: 5′-tccatgacgttcctgacgtt-3′), and 5*μ*g/mL non–CpG-ODN (5′-tccatgagcttcctgagctt-3′). Liver cells were fractionated into 4 cell populations (hepatocytes, Kupffer cells, endothelial cells, and HSCs) as described.[19]

Assessment of Cell Death

Apoptosis and necrosis were determined with the use of Hoechst33342 (Invitrogen, San Diego, CA) and propidium iodide staining as described.[21]

Adenoviruses

For measurement of NF-*κ*B activation, a recombinant adenovirus expressing a luciferase reporter gene driven by NF-*κ*B activation was used.[11,24] To inhibit NF-*κ*B activation, a recombinant adenovirus expressing inhibitor of NF-*κ*B (I*κ*B) super-repressor was used.[11,21,24]

Measurement for IL-1β

Enzyme-linked immunoabsorbent assay kit (R&D Systems, Minneapolis, MN) was used for measuring IL-1*β* in serum and supernatant.

Western Blot Analysis

Supernatant or protein extracts (20 *μ*L) were electrophoresed and then blotted. Blots were incubated with antibody for tissue inhibitor of metalloproteinase-1 (TIMP1; R&D Systems) or IL-1R–associated kinase M (IRAK-M; Cell Signaling Technology Inc, Danvers, MA).[11,24]

Statistical Analysis

Differences between the 2 groups were compared with Mann-Whitney *U* test. Differences between multiple groups were compared with 1-way analysis of variance (GraphPad Prism 4.02; GraphPad Software Inc, San Diego, CA). A *P* value of <.05 was considered significant.

Results

TLR9 Signaling Induces Steatohepatitis and Fibrosis

We investigated the contribution of TLR9 in a murine model of NASH. WT and TLR9$^{-/-}$ mice were fed a CDAA or control CSAA diet for 22 weeks. WT mice had marked lipid accumulation with inflammatory cell infiltration, hepatocyte death, and liver fibrosis (Figure 1A–C; Supplementary Figure 1) after CDAA diet feeding. In contrast, TLR9$^{-/-}$ mice had a significant reduction of steatosis, inflammation, and fibrosis compared with WT mice (Figure 1*A*–*C*). No significant differences were observed in food intake between WT and

TLR9$^{-/-}$ mice (Supplementary Figure 2). The NAFLD activity score, as determined by the degree of steatosis, inflammation, and ballooning, was significantly lower in TLR9$^{-/-}$ mice than in WT mice (total score, WT vs TLR9$^{-/-}$ mice = 6.5 vs 2.6; $P < .01$) (Figure 1*D*).[22] Reduced steatosis and liver injury in TLR9$^{-/-}$ mice were confirmed by lower levels of hepatic triglyceride and serum alanine transaminase (ALT; Figure 1*E*). In accordance with reduced liver fibrosis examined by Sirius red staining, mRNA levels of collagen α1(I), collagen α1(IV), TIMP1, plasminogen activator inhibitor-1 (PAI-1), and transforming growth factor β (TGFβ) were markedly suppressed in TLR9$^{-/-}$ mice (Figure 1*F*). These results suggest that TLR9 signaling is required for the progression of NASH.

Kupffer Cell–Derived IL-1β Is Suppressed in TLR9$^{-/-}$ Mice

To determine the key molecules responsible for the attenuated steatohepatitis in TLR9$^{-/-}$ mice, we examined hepatic mRNA expression of inflammatory cytokines, including tumor necrosis factor α (TNFα), IL-6, IL-1α and IL-1β, mRNA levels of inflammatory cytokines in mice deficient in MyD88, an adaptor molecule for TLR9 signaling, were completely suppressed after CDAA diet feeding (Figure 2*A*). Among these inflammatory cytokines, the IL-1β mRNA level was significantly suppressed in TLR9$^{-/-}$ mice (Figure 2*A*). TLR9$^{-/-}$ mice showed a similar reduction of the serum IL-1β level of MyD88$^{-/-}$ mice (Figure 2*B*), suggesting that TLR9-dependent MyD88-mediated IL-1β is an important factor in the progression of NASH.

Because Kupffer cells are a primary source of IL-1β in some models of liver injury,[25,26] we determined the role of Kupffer cells in IL-1β production. Intravenous injection of liposomal clodronate exclusively depleted Kupffer cells, but not HSCs or sinusoidal endothelial cells (Supplementary Figure 3). IL-1β levels were significantly reduced at 1 week after the liposomal clodronate injection after 21 weeks on the CDAA diet (Figure 2*C*). In addition, we isolated hepatocytes, Kupffer cells, HSCs, and sinusoidal endothelial cells from WT mice after 22 weeks on the CDAA diet. High levels of IL-1β mRNA expression were observed only in the Kupffer cell fraction (Figure 2*D*). These data indicate that Kupffer cells are the main source of IL-1β in the CDAA diet.

Next, we tested whether a CpG-containing ODN, a synthetic TLR9 ligand, induces IL-1β production in Kupffer cells. A CpG-ODN up-regulated IL-1β mRNA in WT Kupffer cells but not in TLR9$^{-/-}$ or MyD88$^{-/-}$ Kupffer cells (Figure 2*E*). On activating caspase-1 with adenosine triphosphate (ATP),[27] WT Kupffer cells secrete the active form of IL-1β (Figure 2*E*). In contrast, CpG-ODN did not induce IL-1β mRNA in either HSCs or hepatocytes isolated from WT mice, and the active form of IL-1β was not detected in culture supernatant from HSCs and hepatocytes (data not shown). These results indicate that IL-1β is primarily produced from Kupffer cells through TLR9 in NASH induced by the CDAA diet.

IL-1β Enhances Lipid Accumulation and Hepatocyte Injury

To determine the effect of IL-1β on NASH, we examined whether IL-1β affects lipid metabolism in hepatocytes. IL-1β increased lipid droplet and triglyceride content in WT and TLR9$^{-/-}$ -cultured hepatocytes, but not IL-1R$^{-/-}$ hepatocytes (Figure 3*A* and *B*). mRNA expression of diacylglycerol acyltransferase 2 (DGAT2), an enzyme that converts

diglyceride to triglyceride, was up-regulated in WT and TLR9$^{-/-}$ hepatocytes, but not in IL-1R$^{-/-}$ hepatocytes, after IL-1β treatment (Figure 3*C*). These results indicate that IL-1β induces lipid accumulation in hepatocytes.

Next, we investigated the contribution of IL-1β to hepatocyte death. In hepatocytes isolated from mice fed the CSAA diet, IL-1β did not induce cell death (Figure 3*D, right*). However, IL-1β increased apoptosis and necrosis in lipid-accumulated hepatocytes isolated from mice fed the CDAA diet (Figure 3*D, left* and *right*). In response to IL-1β, ALT and lactate dehydrogenase (LDH) levels were elevated in supernatant from hepatocytes of mice fed the CDAA diet but not hepatocytes of mice fed the CSAA diet (Figure 3*E*). IL-1β increased the expression of antiapoptotic gene *Bcl2*, but not proapoptotic gene *Bax*, in hepatocytes of mice fed the CSAA diet. Importantly, *Bax*, but not *Bcl2*, expression was up-regulated in hepatocytes of mice fed the CDAA diet after IL-1β treatment (Figure 3*F, left*). NF-κB activation has an essential anti-apoptotic effect in hepatocytes.[21] IL-1β increased NF-κB activation in hepatocytes of mice fed the CSAA diet. Notably, NF-κB activation was blunted in hepatocytes of mice fed the CDAA diet after IL-1β treatment (Figure 3*F, right*). To determine the direct role of NF-κB in cell death induced by IL-1β, NF-κB activation was inhibited by an IκB super-repressor in hepatocytes. With the inhibition of NF-κB activation, IL-1β increased hepatocyte apoptosis and the levels of ALT and LDH (Supplementary Figure 4*A–C*), indicating that NF-κB inactivation is crucial for determining the susceptibility of cell death in lipid-accumulated hepatocytes.

We also tested the direct effect of TLR9 signaling on hepatocytes. However, CpG-ODN had little effect on lipid accumulation and cell death in either normal hepatocytes or lipid-accumulated hepatocytes (Supplementary Figure 5*A–J*). These results indicate that IL-1β mediates lipid accumulation and cell death in hepatocytes during NASH.

IL-1β Promotes the Activation of HSCs

Next, we examined whether IL-1β mediates fibrogenic responses in HSCs, the main precursors of myofibroblasts in the liver. IL-1β markedly elevated the mRNA and protein levels of TIMP1 in WT and TLR9$^{-/-}$ HSCs but not IL-1R$^{-/-}$ HSCs (Figure 4*A*). IL-1β increased collagen α1(I), collagen α1(IV), and PAI-1 mRNA and suppressed mRNA expression of Bambi, a pseudoreceptor for TGFβ,[11] that functions as a negative regulator of TGFβ signaling in hepatic fibrosis (Figure 4*B–D*). Although previous studies had reported that CpG-ODN induced fibrogenic responses in HSCs,[15,17] our study shows that CpG-ODN has little effect on fibrogenic gene expression and NF-κB activation (Supplementary Figure 6). To determine the functional role of IL-1β secreted from Kupffer cells, HSCs were incubated with conditioned medium derived from Kupffer cells treated with CpG- or non–CpG-ODN. Conditioned medium from cells treated with CpG-ODN, but not with non–CpG-ODN, increased TIMP1 and PAI-1 levels in WT and TLR9$^{-/-}$ HSCs. Notably, IL-1R$^{-/-}$ HSCs did not increase TIMP1 and PAI-1 levels in response to CpG-ODN–treated conditioned medium (Figure 4*E*). These results suggest that TLR9-mediated IL-1β released from Kupffer cells is essential for HSC activation.

IL-1R$^{-/-}$ Mice Exhibit Reduced Steatosis, Hepatocyte Damage, and Fibrosis

To confirm the critical role of IL-1R signaling in NASH, IL-1R$^{-/-}$ mice were fed a CDAA diet for 22 weeks. IL-1R$^{-/-}$ mice exhibited less steatosis, apoptosis, and liver fibrosis (Figure 5*A*–*C*). The NAFLD activity score in IL-1R$^{-/-}$ mice was significantly lower than that in WT mice (total score, WT vs IL-1R$^{-/-}$ mice = 6.5 vs 4.6; $P < .05$); in particular, the scores for steatosis and hepatocyte ballooning but not inflammatory cell infiltration were smaller in IL-1R$^{-/-}$ mice (Figure 5*D*). Reduced steatosis was shown by decreased hepatic triglyceride content (Figure 5*E*). ALT levels were lower in IL-1R$^{-/-}$ mice (Figure 5*E*). Reduced liver fibrosis was confirmed by decreased mRNA levels of collagen α1(I), collagen α1(IV), TIMP1, and PAI-1 (Figure 5*F*). These findings indicate that IL-1R signaling contributes to steatosis, hepatocyte damage, and fibrosis.

MyD88 Is a Critical Component for the Development of Steatohepatitis and Fibrosis

Because TLR9 and IL-1R signaling share the adaptor molecule MyD88, we investigated the role of MyD88 in NASH. Steatosis, inflammation, apoptosis, and fibrosis were remarkably inhibited in MyD88$^{-/-}$ mice fed a CDAA diet (Figure 6*A*–*C*). The NAFLD activity score was significantly lower in MyD88$^{-/-}$ mice (total score, WT vs MyD88$^{-/-}$ = 6.5 vs 2.0; $P < .01$), and every score was significantly less than that in WT mice (Figure 6*D*). Hepatic triglyceride and serum ALT levels were markedly reduced in MyD88$^{-/-}$ mice (Figure 6*E*). In addition, MyD88$^{-/-}$ mice had decreased mRNA levels of collagen α1(I), collagen α1(IV), TIMP-1, and PAI-1 (Figure 6*F*). These results implicate MyD88 as a crucial signaling molecule that promotes NASH and fibrosis.

TLR9 Signaling Mediates Insulin Resistance Induced by CDAA Diet

Insulin resistance is observed in most patients with NASH.[2] Therefore, we assessed HOMA-IR levels in TLR9$^{-/-}$, IL-1R$^{-/-}$, and MyD88$^{-/-}$ mice. A significant reduction of HOMA-IR was seen in TLR9$^{-/-}$ mice compared with that in WT mice receiving a CDAA diet (Figure 7). Furthermore, HOMA-IR was not increased in IL-1R$^{-/-}$ and MyD88$^{-/-}$ mice on a CDAA or CSAA diet compared with that in mice fed standard chow (Figure 7). These results indicate that TLR9, IL-1R, and MyD88 are crucial for the development of insulin resistance. However, both the CDAA and CSAA diets significantly increased the HOMA-IR level compared with standard chow in WT mice. The CDAA diet feeding resulted in NASH, whereas the CSAA diet feeding produced mild steatosis, indicating that insulin resistance is not correlated with the degree of NASH, which further suggests that insulin resistance may be associated with steatosis, but additional mediators through TLR9, IL-1R, and MyD88 are required for the development of NASH.

Discussion

The present study shows that steatohepatitis is diminished in TLR9$^{-/-}$, IL-1R$^{-/-}$, and MyD88$^{-/-}$ mice. Kupffer cells, but not hepatocytes and HSCs, respond to TLR9 ligands to produce IL-1β. This IL-1β induces lipid accumulation and cell death in hepatocytes and the expression of fibrogenic mediators in HSCs, resulting in steatosis, hepatocyte injury, and fibrosis (Figure 7*B*).

Two possible mechanisms activate innate immune systems in NASH. First, translocated bacteria and their products activate the innate immune network as exogenous ligands in NASH.[7–9,28] In chronic liver disease, including NASH, intestinal permeability is increased because of bacterial overgrowth or altered composition of bacterial microflora.[29] Systemic inflammation related to NASH also injures epithelial tight junctions,[30] resulting in deregulation of intestinal barrier functions. Indeed, plasma levels of LPS are elevated in patients with chronic liver diseases, including NASH.[31] We and others have reported that TLR4, a receptor for LPS, promotes steatohepatitis and fibrosis.[4,8] Bacterial DNA was also detected by PCR for bacterial 16S rRNA in the blood of mice fed a CDAA diet (data not shown), suggesting that translocated bacterial DNA could be an exogenous ligand in NASH. Second, dying hepatocytes in NASH supply denatured host DNA that may activate TLR9 as an endogenous ligand.[16] Thus, exogenous and endogenous TLR9 ligands may activate the innate immune system through TLR9, which results in the development of steatohepatitis, fibrosis, and insulin resistance.

The prominent features of hepatocytes in NASH are excessive lipid accumulation and cell death. We determined that IL-1β promotes lipid accumulation and triglyceride synthesis by up-regulating DGAT2 in hepatocytes. Increased triglyceride accumulation by IL-1β was observed in TLR9$^{-/-}$ hepatocytes in vitro, indicating that lipid accumulation depends on IL-1β, but not TLR9, in hepatocytes. Our data suggest that a low level of IL-1β is associated with reduced lipid accumulation in hepatocytes of TLR9$^{-/-}$ mice. We found that lipid-laden hepatocytes had blunted activation of NF-κB. Meanwhile, the expression of IRAK-M, a negative regulator of IL-1R signaling,[7] was increased in lipid-laden hepatocytes (Supplementary Figure 7). As a result, lipid-laden hepatocytes are sensitive to IL-1β–induced cell death. Previous studies have shown that IL-1R antagonist–deficient mice on a high-fat diet have more severe steatohepatitis.[32] In addition, an IL-1β gene polymorphism is prevalently observed in patients with NASH.[33] These studies are consistent with our conclusion that IL-1β is important for the progression of NASH.

IL-1β contributes to HSC activation by regulating fibrogenic factors. Among IL-1β–mediated profibrogenic factors, HSCs markedly increased the secretion of TIMP1, an inhibitor of matrix metalloproteases,[34] which inhibits degradation of extracellular matrix to promote liver fibrosis. Indeed, transgenic mice overexpressing TIMP1 exhibit severe liver fibrosis induced by the treatment of carbon tetrachloride,[35] and treatment with a neutralizing anti-TIMP1 antibody attenuates liver fibrosis.[34] Moreover, TIMP1 inhibits HSC apoptosis.[36] IL-1β induced other fibrogenic factors, including PAI-1, collagen, and decreased the expression of Bambi, a pseudoreceptor for TGFβ. Thus, IL-1β plays an important role in fibrogenic responses in NASH. Although HSCs have been reported to be targets for TLR9 ligands,[15,17] primary cultured HSCs barely responded to CpG-ODN in comparison to IL-1β in our study (Supplementary Figure 6). However, conditioned medium derived from CpG-ODN–treated Kupffer cells strongly induced TIMP-1 expression in WT, but not IL-1R$^{-/-}$ HSCs (Figure 4*E*). These findings further confirmed our hypothesis that the critical mediator for HSC activation is IL-1 released from Kupffer cells.

Multiple TLRs and inflammatory cytokines mediate NASH. TLR4 promotes NASH by producing inflammatory cytokines, including TNF-α and IL-1β.[4] A synergistic interaction of

TLR4 and TLR9 induces the highest expression of TNF-α,[37,38] but it has not been reported in the IL-1β production. Notably, TLR4 strongly activates caspase-1 that processes the proform of IL-1β to active IL-1β independently of ATP in Kupffer cells.[39,40] We suggest that TLR4 activates caspase-1 that cooperates with TLR9 to induce the active IL-1β in Kupffer cells. Then, IL-1β promotes lipid accumulation and cell death in hepatocytes and fibrogenic responses in HSCs (Figures 3 and 4). However, IL-1R$^{-/-}$ mice had less of a reduction in liver injury, steatosis, and fibrosis than did MyD88$^{-/-}$ mice (Figures 5 and 6). TNF-α may also contribute to the development of NASH in IL-1R$^{-/-}$ mice, because TNF-α is increased to similar levels in IL-1R$^{-/-}$ and WT mice (data not shown) but lower in MyD88$^{-/-}$ mice. TNF-α is fibrogenic, by increasing TIMP-1[41] and decreasing Bambi expression in HSCs (data not shown).

Clinically, insulin resistance is strongly associated with the degree of NASH.[42–47] However, recent studies have shown that an I148M mutation in patatin-like phospholipase domain-containing 3 protein (PNPLA3)/adiponutrin is associated with increased hepatic triglyceride content and ALT levels but independent of insulin resistance.[48–51] In our study, both CSAA and CDAA diets induced a similar degree of insulin resistance as measured by HOMA-IR (Figure 7). The CDAA diet resulted in a significant steatosis, inflammation, and fibrosis (Supplementary Figure 1; Supplementary Table 1), whereas the CSAA control diet led to a more modest degree of steatosis without inflammation and fibrosis (Supplementary Figure 1; Supplementary Table 1). These findings suggest that insulin resistance may be associated with some degree of steatosis but that the magnitude of the decreased insulin sensitivity in the current studies (Figure 7) is insufficient to cause NASH.

Overall, the CDAA diet is a useful model to investigate NASH. The CDAA diet induces fibrosis, systemic insulin resistance, and weight gain in addition to steatohepatitis (Figure 7; Supplementary Figure 1; Supplementary Table 1). These findings are compatible to the pathophysiology of human NASH. So far, 2 diet models are widely used for the study of steatohepatitis in rodents: high-fat diet and methionine and choline deficient (MCD) diet. A high-fat diet induces weight gain and systemic insulin resistance as in most cases of human NASH. However, the high-fat diet induces steatosis, but not inflammation and fibrosis. The MCD diet is most widely used for studying NASH. However, mice fed the MCD diet have weight loss without insulin resistance.[2,52]

In summary, we demonstrate a novel role for the innate immune system in mediating NASH. TLR9-MyD88 signaling mediates IL-1β production in Kupffer cells, which stimulates both hepatocytes and HSCs leading to the progression of NASH. Thus, the present study provides TLR9, MyD88, and IL-1β as a potential target for the therapy of NASH.

Supplementary Material

Refer to Web version on PubMed Central for supplementary material.

Acknowledgments

The authors thank Dr Shizuo Akira (Osaka University, Japan) for the generous gift of TLR9$^{-/-}$ and MyD88$^{-/-}$ mice and Dr Katsumi Miyai (Department of Pathology at UCSD), Dr Wuqiang Fan, Dr Saswata Talukdar, Rie Seki, and Karin Diggle (Department of Medicine at UCSD) for excellent technical assistance.

Funding

This study was supported by a Liver Scholar Award from the American Association for the Study of Liver Diseases/American Liver Foundation and by a pilot project from the Southern California Research Center for ALPD and Cirrhosis (P50 AA11999) funded by NIAAA (both to E.S.), NIH grants 5R01GM041804 and 5R01DK072237 (D.A.B.), and Takeda Science Foundation (K.M.).

Abbreviations used in this paper

ALT	alanine transaminase
ATP	adenosine triphosphate
CDAA	choline-deficient amino-acid defined
CpG	cytosine phosphate guanine
CSAA	choline-supplemented amino acid defined
DGAT2	diacylglycerol acyltransferase 2
HOMA-IR	homeostasis model assessment of insulin resistance
HSC	hepatic stellate cell
IκB	inhibitor of NF-κB
IL-1β	interleukin-1β
IL-1R	interleukin-1 receptor
IRAK-M	interleukin-1 receptor-associated kinase M
LDH	lactate dehydrogenase
MCD	methionine and choline deficient
NAFLD	non-alcoholic fatty liver disease
NASH	nonalcoholic steatohepatitis
NF-κB	nuclear factor-κB
NIH	National Institutes of Health
ODN	oligodeoxynucleotide
PAI-1	plasminogen activator inhibitor-1
PCR	polymerase chain reaction
TGFβ	transforming growth factor β
TIMP1	tissue inhibitor of metalloproteinase-1
TLR	Toll-like receptor

TNFα	tumor necrosis factor α
TUNEL	TdT (terminal deoxynucleotidyl-transferase)–mediated dUTP (2-deoxyuridine 5-triphosphate)– biotin neck end labeling
WT	wild-type

References

1. Browning JD, Horton JD. Molecular mediators of hepatic steatosis and liver injury. J Clin Invest. 2004; 114:147–152. [PubMed: 15254578]
2. Marra F, Gastaldelli A, Svegliati Baroni G, et al. Molecular basis and mechanisms of progression of non-alcoholic steatohepatitis. Trends Mol Med. 2008; 14:72–81. [PubMed: 18218340]
3. Maher JJ, Leon P, Ryan JC. Beyond insulin resistance: innate immunity in nonalcoholic steatohepatitis. Hepatology. 2008; 48:670–678. [PubMed: 18666225]
4. Rivera CA, Adegboyega P, van Rooijen N, et al. Toll-like receptor-4 signaling and Kupffer cells play pivotal roles in the pathogenesis of non-alcoholic steatohepatitis. J Hepatol. 2007; 47:571–579. [PubMed: 17644211]
5. Bataller R, Brenner DA. Liver fibrosis. J Clin Invest. 2005; 115:209–218. [PubMed: 15690074]
6. Friedman SL. Mechanisms of hepatic fibrogenesis. Gastroenterology. 2008; 134:1655–1669. [PubMed: 18471545]
7. Kawai T, Akira S. The roles of TLRs, RLRs and NLRs in pathogen recognition. Int Immunol. 2009; 21:317–337. [PubMed: 19246554]
8. Seki E, Brenner DA. Toll-like receptors and adaptor molecules in liver disease: update. Hepatology. 2008; 48:322–335. [PubMed: 18506843]
9. Szabo G, Dolganiuc A, Mandrekar P. Pattern recognition receptors: a contemporary view on liver diseases. Hepatology. 2006; 44:287–298. [PubMed: 16871558]
10. Naugler WE, Sakurai T, Kim S, et al. Gender disparity in liver cancer due to sex differences in MyD88-dependent IL-6 production. Science. 2007; 317:121–124. [PubMed: 17615358]
11. Seki E, De Minicis S, Osterreicher CH, et al. TLR4 enhances TGF-beta signaling and hepatic fibrosis. Nat Med. 2007; 13:1324–1332. [PubMed: 17952090]
12. Hemmi H, Takeuchi O, Kawai T, et al. A Toll-like receptor recognizes bacterial DNA. Nature. 2000; 408:740–745. [PubMed: 11130078]
13. Frances R, Zapater P, Gonzalez-Navajas JM, et al. Bacterial DNA in patients with cirrhosis and noninfected ascites mimics the soluble immune response established in patients with spontaneous bacterial peritonitis. Hepatology. 2008; 47:978–985. [PubMed: 18306221]
14. Guarner C, Gonzalez-Navajas JM, Sanchez E, et al. The detection of bacterial DNA in blood of rats with CCl4-induced cirrhosis with ascites represents episodes of bacterial translocation. Hepatology. 2006; 44:633–639. [PubMed: 16941689]
15. Watanabe A, Hashmi A, Gomes DA, et al. Apoptotic hepatocyte DNA inhibits hepatic stellate cell chemotaxis via toll-like receptor 9. Hepatology. 2007; 46:1509–1518. [PubMed: 17705260]
16. Imaeda AB, Watanabe A, Sohail MA, et al. Acetaminophen-induced hepatotoxicity in mice is dependent on Tlr9 and the Nalp3 inflammasome. J Clin Invest. 2009; 119:305–314. [PubMed: 19164858]
17. Gabele E, Muhlbauer M, Dorn C, et al. Role of TLR9 in hepatic stellate cells and experimental liver fibrosis. Biochem Biophys Res Commun. 2008; 376:271–276. [PubMed: 18760996]
18. Adachi O, Kawai T, Takeda K, et al. Targeted disruption of the MyD88 gene results in loss of IL-1- and IL-18-mediated function. Immunity. 1998; 9:143–150. [PubMed: 9697844]
19. Kodama Y, Kisseleva T, Iwaisako K, et al. c-Jun N-terminal kinase-1 from hematopoietic cells mediates progression from hepatic steatosis to steatohepatitis and fibrosis in mice. Gastroenterology. 2009; 137:1467–1477. e5. [PubMed: 19549522]

20. Van Rooijen N, Sanders A. Liposome mediated depletion of macrophages: mechanism of action, preparation of liposomes and applications. J Immunol Methods. 1994; 174:83–93. [PubMed: 8083541]
21. Kodama Y, Taura K, Miura K, et al. Antiapoptotic effect of c-Jun N-terminal Kinase-1 through Mcl-1 stabilization in TNF-induced hepatocyte apoptosis. Gastroenterology. 2009; 136:1423–1434. [PubMed: 19249395]
22. Kleiner DE, Brunt EM, Van Natta M, et al. Design and validation of a histological scoring system for nonalcoholic fatty liver disease. Hepatology. 2005; 41:1313–1321. [PubMed: 15915461]
23. Matthews DR, Hosker JP, Rudenski AS, et al. Homeostasis model assessment: insulin resistance and beta-cell function from fasting plasma glucose and insulin concentrations in man. Diabetologia. 1985; 28:412–4129. [PubMed: 3899825]
24. Miura K, Yoshino R, Hirai Y, et al. Epimorphin, a morphogenic protein, induces proteases in rodent hepatocytes through NF-kappaB. J Hepatol. 2007; 47:834–843. [PubMed: 17935821]
25. Bilzer M, Roggel F, Gerbes AL. Role of Kupffer cells in host defense and liver disease. Liver Int. 2006; 26:1175–1186. [PubMed: 17105582]
26. Ramadori G, Armbrust T. Cytokines in the liver. Eur J Gastroenterol Hepatol. 2001; 13:777–784. [PubMed: 11474306]
27. Mariathasan S, Newton K, Monack DM, et al. Differential activation of the inflammasome by caspase-1 adaptors ASC and Ipaf. Nature. 2004; 430:213–218. [PubMed: 15190255]
28. Brun P, Castagliuolo I, Di Leo V, et al. Increased intestinal permeability in obese mice: new evidence in the pathogenesis of nonalcoholic steatohepatitis. Am J Physiol Gastrointest Liver Physiol. 2007; 292:G518–G525. [PubMed: 17023554]
29. Wu WC, Zhao W, Li S. Small intestinal bacteria overgrowth decreases small intestinal motility in the NASH rats. World J Gastroenterol. 2008; 14:313–317. [PubMed: 18186574]
30. Miele L, Valenza V, La Torre G, et al. Increased intestinal permeability and tight junction alterations in nonalcoholic fatty liver disease. Hepatology. 2009; 49:1877–1887. [PubMed: 19291785]
31. Farhadi A, Gundlapalli S, Shaikh M, et al. Susceptibility to gut leakiness: a possible mechanism for endotoxaemia in non-alcoholic steatohepatitis. Liver Int. 2008; 28:1026–1033. [PubMed: 18397235]
32. Isoda K, Sawada S, Ayaori M, et al. Deficiency of interleukin-1 receptor antagonist deteriorates fatty liver and cholesterol metabolism in hypercholesterolemic mice. J Biol Chem. 2005; 280:7002–7009. [PubMed: 15574426]
33. Nozaki Y, Saibara T, Nemoto Y, et al. Polymorphisms of interleukin-1 beta and beta 3-adrenergic receptor in Japanese patients with nonalcoholic steatohepatitis. Alcohol Clin Exp Res. 2004; 28(8 suppl proc):106S–110S. [PubMed: 15318095]
34. Parsons CJ, Bradford BU, Pan CQ, et al. Antifibrotic effects of a tissue inhibitor of metalloproteinase-1 antibody on established liver fibrosis in rats. Hepatology. 2004; 40:1106–1115. [PubMed: 15389776]
35. Yoshiji H, Kuriyama S, Miyamoto Y, et al. Tissue inhibitor of metalloproteinases-1 promotes liver fibrosis development in a transgenic mouse model. Hepatology. 2000; 32:1248–1254. [PubMed: 11093731]
36. Yoshiji H, Kuriyama S, Yoshii J, et al. Tissue inhibitor of metal-loproteinases-1 attenuates spontaneous liver fibrosis resolution in the transgenic mouse. Hepatology. 2002; 36:850–860. [PubMed: 12297832]
37. Dalpke AH, Lehner MD, Hartung T, et al. Differential effects of CpG-DNA in Toll-like receptor-2/-4/-9 tolerance and cross-tolerance. Immunology. 2005; 116:203–212. [PubMed: 16162269]
38. De Nardo D, De Nardo CM, Nguyen T, et al. Signaling crosstalk during sequential TLR4 and TLR9 activation amplifies the inflammatory response of mouse macrophages. J Immunol. 2009; 183:8110–8118. [PubMed: 19923461]
39. Seki E, Tsutsui H, Nakano H, et al. Lipopolysaccharide-induced IL-18 secretion from murine Kupffer cells independently of myeloid differentiation factor 88 that is critically involved in

induction of production of IL-12 and IL-1beta. J Immunol. 2001; 166:2651–2657. [PubMed: 11160328]

40. Imamura M, Tsutsui H, Yasuda K, et al. Contribution of TIR domain-containing adapter inducing IFN-beta-mediated IL-18 release to LPS-induced liver injury in mice. J Hepatol. 2009; 51:333–341. [PubMed: 19501931]
41. Inokuchi S, Aoyama T, Miura K, et al. Disruption of TAK1 in hepatocytes causes hepatic injury, inflammation, fibrosis, and carcinogenesis. Proc Natl Acad Sci U S A. 2010; 107:844–849. [PubMed: 20080763]
42. Chitturi S, Abeygunasekera S, Farrell GC, et al. NASH and insulin resistance: insulin hypersecretion and specific association with the insulin resistance syndrome. Hepatology. 2002; 35:373–379. [PubMed: 11826411]
43. Chitturi S, Farrell G, Frost L, et al. Serum leptin in NASH correlates with hepatic steatosis but not fibrosis: a manifestation of lipotoxicity? Hepatology. 2002; 36:403–409. [PubMed: 12143049]
44. Fartoux L, Chazouilleres O, Wendum D, et al. Impact of steatosis on progression of fibrosis in patients with mild hepatitis C. Hepatology. 2005; 41:82–87. [PubMed: 15690484]
45. Camma C, Bruno S, Di Marco V, et al. Insulin resistance is associated with steatosis in nondiabetic patients with genotype 1 chronic hepatitis C. Hepatology. 2006; 43:64–71. [PubMed: 16374856]
46. Ota T, Takamura T, Kurita S, et al. Insulin resistance accelerates a dietary rat model of nonalcoholic steatohepatitis. Gastroenterology. 2007; 132:282–293. [PubMed: 17241878]
47. Sakurai M, Takamura T, Ota T, et al. Liver steatosis, but not fibrosis, is associated with insulin resistance in nonalcoholic fatty liver disease. J Gastroenterol. 2007; 42:312–317. [PubMed: 17464461]
48. Romeo S, Kozlitina J, Xing C, et al. Genetic variation in PNPLA3 confers susceptibility to nonalcoholic fatty liver disease. Nat Genet. 2008; 40:1461–1465. [PubMed: 18820647]
49. Kantartzis K, Peter A, Machicao F, et al. Dissociation between fatty liver and insulin resistance in humans carrying a variant of the patatin-like phospholipase 3 gene. Diabetes. 2009; 58:2616–2623. [PubMed: 19651814]
50. He S, McPhaul C, Li JZ, et al. A sequence variation (I148M) in PNPLA3 associated with nonalcoholic fatty liver disease disrupts triglyceride hydrolysis. J Biol Chem. 2010; 285:6706–6715. [PubMed: 20034933]
51. Valenti L, Al-Serri A, Daly AK, et al. Homozygosity for the patatin-like phospholipase-3/adiponutrin I148M polymorphism influences liver fibrosis in patients with nonalcoholic fatty liver disease. Hepatology. 2010; 51:1209–1217. [PubMed: 20373368]
52. Anstee QM, Goldin RD. Mouse models in non-alcoholic fatty liver disease and steatohepatitis research. Int J Exp Pathol. 2006; 87:1–16. [PubMed: 16436109]

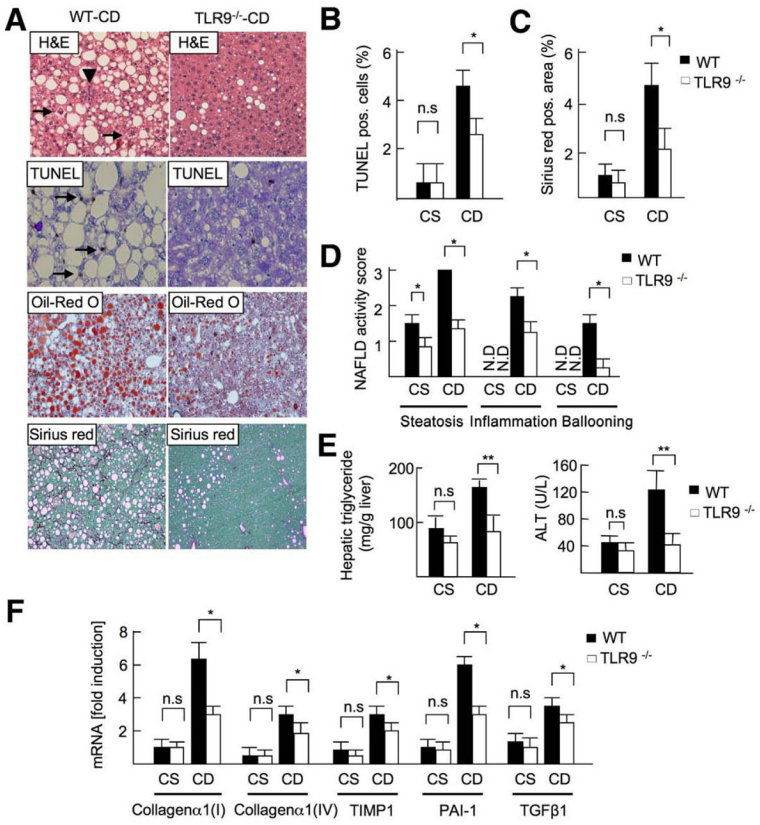

Figure 1.

TLR9 deficiency attenuates steatohepatitis. WT and TLR9$^{-/-}$ mice were fed a CSAA (CS; n = 4) or CDAA (CD; n = 8) diet for 22 weeks. *Closed bar*, WT mice; *open bar*, TLR9$^{-/-}$ mice. (*A*) Liver sections were stained with H&E (*arrowheads*, inflammatory cells; *arrows*, ballooning hepatocytes), Oil-Red O, TUNEL (*arrows*; apoptotic cells), and Sirius red. Original magnification, ×200 for H&E and TUNEL staining, ×100 for Oil-Red O and Sirius red stainings. (*B*) Number of TUNEL-positive cells, (*C*) Sirius red–positive area and (*D*) NAFLD activity score were calculated. N.D., not detected. (*E*) Hepatic triglyceride and serum ALT levels were measured. (*F*) Hepatic mRNA levels of fibrogenic markers were determined by quantitative real-time PCR. Data represent mean ± SD; **P* < .05; n.s., not significant.

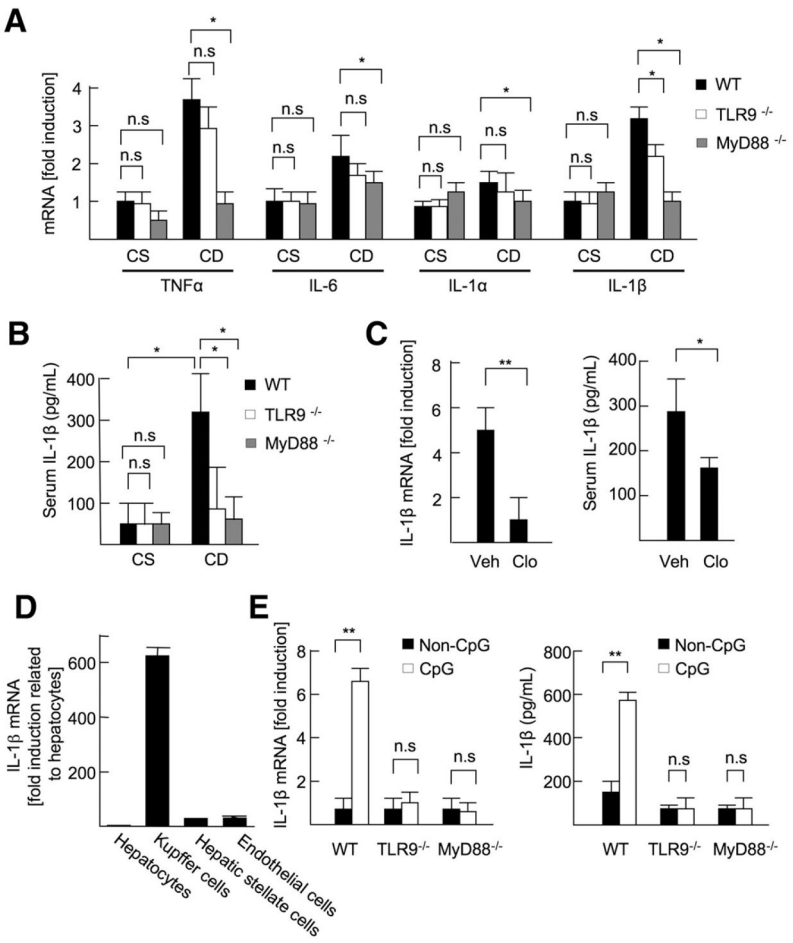

Figure 2.

TLR9 induces IL-1β production in Kupffer cells. (*A* and *B*) The livers and sera were harvested from 22-week-old CSAA (CS) or CDAA (CD) diet-fed WT, TLR9$^{-/-}$, and MyD88$^{-/-}$ mice. (*A*) Hepatic mRNA levels of inflammatory cytokines were measured by quantitative real-time PCR (qPCR). (*B*) Serum IL-1β levels were measured by enzyme-linked immunoabsorbent assay (ELISA). (*C*) WT mice (21 weeks old) fed the CDAA diet were injected control (Veh; n = 6) or clodronate liposome (Clo; n = 6) to deplete Kupffer cells. The livers and sera were harvested 1 week after the liposome injection. Hepatic mRNA and serum protein levels of IL-1β were measured by qPCR and ELISA, respectively. (*D*) IL-1β mRNA expression in hepatocytes, Kupffer cells, HSCs, and sinusoidal endothelial cells was measured by qPCR. (*E*) WT, TLR9$^{-/-}$, and MyD88$^{-/-}$ Kupffer cells were treated with 5 μg/mL CpG-ODN or non–CpG-ODN, and then IL-1β mRNA levels were measured by qPCR. To convert active IL-1β from proIL-1β, Kupffer cells were treated with 2 mmol/L ATP for 30 minutes after 24 hours of incubation with 5 μg/mL CpG-ODN (n = 4, each group), and then secreted IL-1β levels were measured by ELISA. Data represent mean ± SD; **P* < .05, ***P* < .01; n.s., not significant.

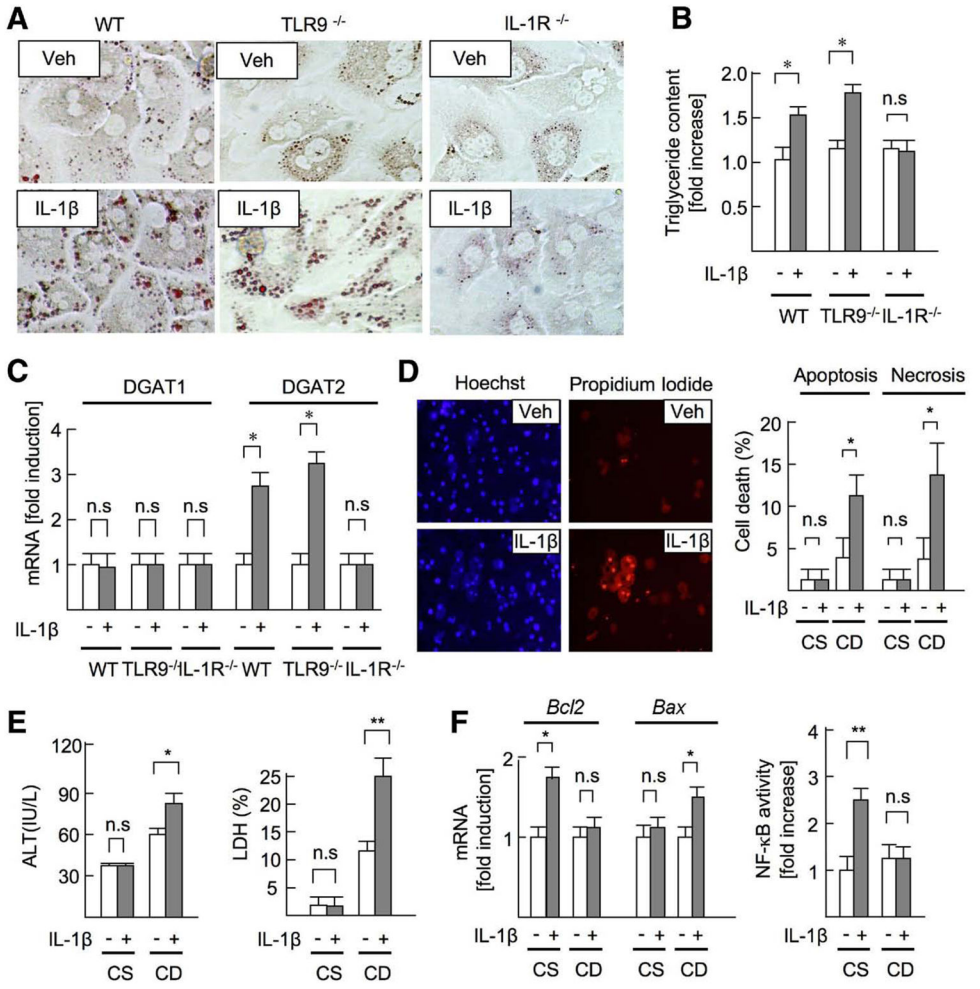

Figure 3.

IL-1β promotes lipid metabolism and cell death in hepatocytes. (*A–C*) WT, TLR9$^{-/-}$, and IL-1R$^{-/-}$ hepatocytes were treated with 10 ng/mL IL-1β. Veh, vehicle. (*A*) Lipid accumulation (Oil-Red O staining) and (*B*) triglyceride content (normalized to protein concentration) were measured in WT, TLR9$^{-/-}$, and IL-1R$^{-/-}$ hepatocytes treated with IL-1β for 24 hours. (*C*) Hepatocytes were treated with IL-1β for 8 hours. mRNA expression of DGATs in hepatocytes was determined by quantitative real-time PCR (qPCR). (*D–F*) Hepatocytes were isolated from 22-week-old mice fed the CSAA (CS) or the CDAA (CD) diet. (*D*) Hepatocytes were treated with IL-1β for 24 hours. Apoptosis and necrosis were determined by Hoechst33342 and propidium iodide, respectively. (*E*) ALT and LDH levels in supernatant were measured. (*F, left*) mRNA levels of *Bcl2* and *Bax* were determined by qPCR. (*F, right*) NF-κB activity in response to IL-1β was examined by NF-κB–reporter assay. Data represent mean ± SD; **P* < .05, ***P* < .01; n.s., not significant. Original magnification, ×400 (*A*), ×200 (C).

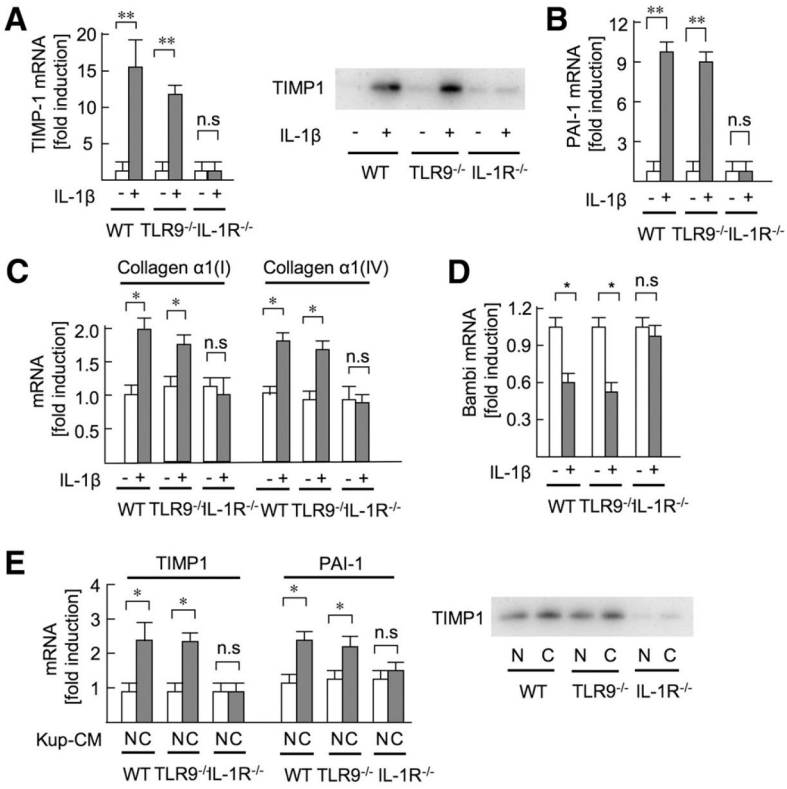

Figure 4.

Kupffer cell–derived IL-1*β* promotes HSC activation. (*A–D*) HSCs isolated from WT, TLR9$^{-/-}$, and IL-1R$^{-/-}$ mice were stimulated with 10 ng/mL IL-1*β* for 8 hours to measure mRNA expression of TIMP1 (*A*), PAI-1 (*B*), collagen (*C*), and Bambi (*D*) by quantitative real-time PCR (qPCR), and for 24 hours to determine TIMP1 expression in the supernatant by Western blot (*A*). (*E*) Kupffer cell–conditioned medium (Kup-CM) was prepared by treating Kupffer cells with 5 *μ*g/mL CpG-ODN or non–CpG-ODN for 24 hours. Then, WT, TLR9$^{-/-}$, and IL-1R$^{-/-}$ HSCs were treated with Kup-CM for 8 hours to determine mRNA expression of fibrogenic markers by qPCR (*E, left*) and for 24 hours to determine TIMP1 protein expression in the supernatant (*E, right*). Data represent mean ± SD; **P* < .05, ***P* < .01; n.s., not significant.

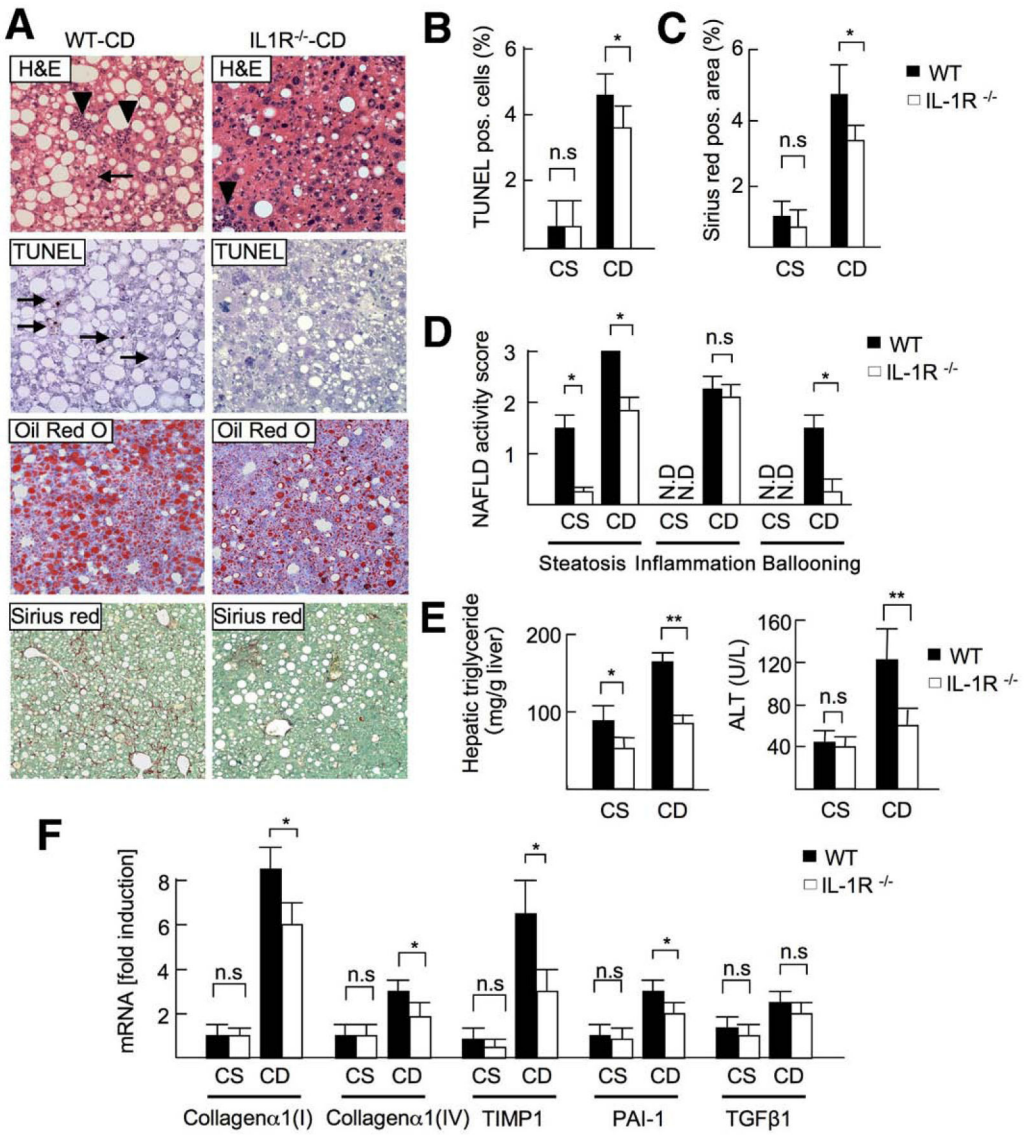

Figure 5.

IL-1R$^{-/-}$ mice show attenuated steatosis and fibrosis. WT and IL-1R$^{-/-}$ mice were fed a CSAA diet (CS; n = 4) or CDAA diet (CD; n = 8) for 22 weeks. *Closed bar*, WT mice; *open bar*, IL-1R$^{-/-}$ mice. (*A*) H&E (*arrowheads*, inflammatory cells; *arrows*, ballooning hepatocytes), Oil-Red O, TUNEL (*arrows*; apoptotic cells), and Sirius red staining were performed. Original magnification, ×200 for H&E and TUNEL, ×100 for Oil-Red O and Sirius red. (*B*) Number of TUNEL-positive cells and (*C*) Sirius red–positive area were suppressed in IL-1R$^{-/-}$ mice. (*D*) NAFLD activity score, steatosis, and fibrosis were suppressed in IL-1R$^{-/-}$ mice. N.D., not detected. (*E*) Hepatic triglyceride and serum ALT levels were decreased in IL-1R$^{-/-}$ mice. (*F*) Hepatic mRNA levels of fibrogenic markers were measured by quantitative real-time PCR. Data represent mean ± SD, *$P < .05$; n.s., not significant.

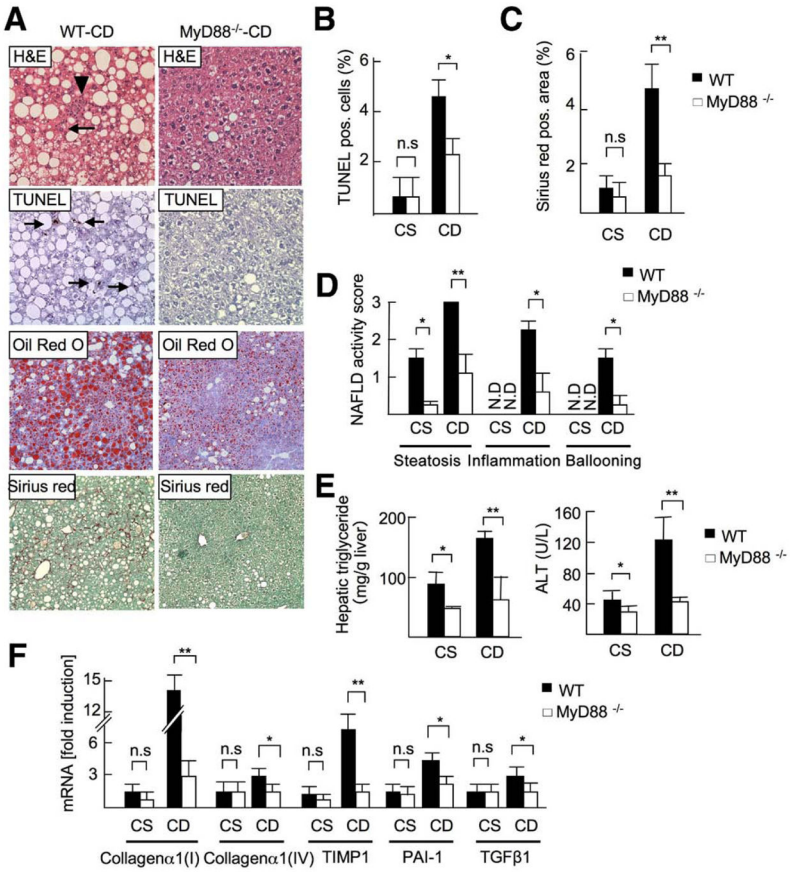

Figure 6.

Gene deletion of MyD88 ameliorates steatohepatitis. WT and MyD88$^{-/-}$ mice were fed a CSAA (CS, n=4) or CDAA (WT-CD, n = 8; MyD88$^{-/-}$ -CD, n = 7) diet for 22 weeks. *Closed bar*, WT mice; *open bar*, MyD88$^{-/-}$ mice. (*A*) H&E (*arrowheads*, inflammatory cells; *arrows*, ballooning hepatocytes), Oil-Red O, TUNEL (*arrows*; apoptotic cells), and Sirius red staining show reduced steatosis, inflammatory cells, apoptosis, and fibrosis in MyD88$^{-/-}$ mice. Original magnification, ×200 for H&E and TUNEL staining, ×100 for Oil-Red O and Sirius red stainings. (*B*) TUNEL-positive cells, (*C*) Sirius red–positive area, and (*D*) NAFLD activity score were suppressed in MyD88$^{-/-}$ mice. N.D., not detected. (*E*) Hepatic triglyceride and serum ALT levels were suppressed in MyD88$^{-/-}$ mice. (*F*) Hepatic mRNA levels of fibrogenic markers were determined by quantitative real-time PCR. Data represent mean ± SD; **P* < .05, ***P* < .01; n.s., not significant.

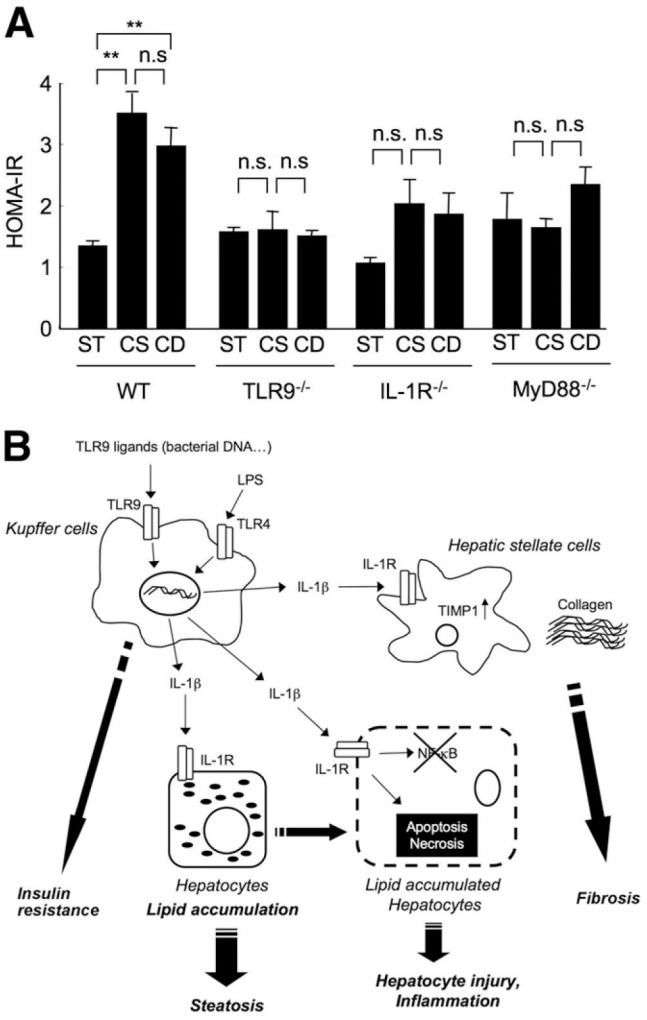

Figure 7.

(*A*) TLR9–MyD88–IL-1R axis promotes insulin resistance. Normal chow (N), CSAA (CS), and CDAA (CD) diets were fed to WT, TLR9$^{-/-}$, IL-1R$^{-/-}$, and MyD88$^{-/-}$ mice for 22 weeks (n = 6, each group). Insulin resistance was examined by HOMA-IR. Data represent mean ± SEM; $^{**}P < .01$; n.s., not significant. (*B*) The proposed mechanism responsible for the development of NASH through TLR9 and IL-1*β*. TLR9 ligands, including bacterial DNA or other endogenous mediators, stimulate Kupffer cells to produce IL-1*β*. Secreted IL-1*β* acts on hepatocytes to increase lipid accumulation and cell death, causing steatosis and inflammation. IL-1*β* also stimulates HSCs to produce fibrogenic factors such as collagen and TIMP-1, resulting in fibrogenesis. Simultaneously, the TLR9-MyD88 axis promotes insulin resistance. TLR4 also contributes to this network in NASH as described previously.[4]